

ENHANCED NUCLEATION AND SMOOTHNESS OF NANOCRYSTALLINE DIAMOND FILMS VIA W-C GRADIENT INTERLAYER

QIUPING WEI^{a,b,†}, ZHIMING YU^{a,*}, LI MA^b, DENG FENG YIN^a

^a*School of Materials Science and Engineering, Central South University,*

^b*Key State Laboratory of Powder Metallurgy, Central South University,
Changsha, 410083, People's Republic of China*

^{*}*zhiming@mail.csu.edu.cn; †qpwei@yahoo.com*

CVD diamond coating was deposited on to 13%wt. Co-containing tungsten cemented carbide surfaces using a hot filament chemical vapor deposition (HFCVD) to improve wear properties and performance of WC-13%wt.Co. Prior to the deposition of the diamond films, a W-C gradient intermediate layer had been sputtered on WC-13%wt.Co. The surface and cross-section morphology, phase transformation, and grain size distribution of the samples were investigated by means of field emission scanning electron microscope (SEM), X-ray diffractometer (XRD), and atomic force microscope (AFM), respectively. The results show that W-C gradient intermediate layers can effectively reduce the diffusion of Co in cemented carbide substrates during diamond deposition process, resulting high nucleation density and ultra smooth nanocrystalline diamond films.

Keywords: Nanodiamond films; cemented carbide; interlayer.

1. Introduction

The extreme hardness of diamond, excellent wear resistance and chemical inertness, make it an ideal candidate for usage in cutting tools for machining non-ferrous metals, wood, plastics, chip-board and composite materials^[1-4]. Indeed, high-pressure high-temperature (HPHT) synthesized diamond has been used for this purpose since the 1960s, and remains a lucrative commercial process today^[5]. CVD diamond is beginning to be used in a similar way, by coating the diamond onto the surface of cutting tools, such as the tungsten carbide inserts and stainless steel tools.

The direct deposition of diamond on WC-Co, however, is difficult due to the presence of cobalt on the cemented carbide surface. The cobalt is detrimental to diamond nucleation and promotes the formation of graphite from the gas phase, that dramatically reduces diamond film adhesion^[6,7]. Various methods were adopted to suppress the effect of cobalt, such as the binder removal (selectively Co etching) of the substrate surface^[8,9] or interposition of suitable diffusion barrier layers^[10-12]. In the work presented in this paper, the W-C gradient intermediate layers acting as buffer layer for Co have been reactive sputtered on WC-13%wt.Co in Ar-CH₄ mixed gases.

2. Experimental Details

2.1. Deposition of W-C gradient interlayers

For this study, WC-13%wt.Co plates, $12 \times 12 \text{ mm}^2$ in area and 5mm in thickness were used as substrates. On these substrates, an approximately $10 \mu\text{m}$ thicknesses W-C gradient interlayer was deposited by reactive magnetron sputtering using W targets (99.95% purity) in mixed atmosphere of methane and argon. The sputtering plant is a CSU550-I coating machine equipped with a magnetron target 60 mm in diameter. The ultimate pressure for all deposition processes was within the range of 3.0~4.4Pa. Ultra pure methane (99.999%) was added as reactive gas to argon (99.999%) in order to form W-C interlayer. The temperature of the substrates was measured with a thermocouple placed in contact with their surface. The distance between the target and the surface of the substrate was set at 70 mm for all depositions in order to get good uniformity in thickness of the films with respect to fair deposition rate.

The temperature of the WC-Co substrates has been set at 400°C , the reasons of choosing such temperature are:

- Most of industrial sputtering devices do not perform deposition temperatures in the range of diamond ones.
- The deposition of diamond requires high CVD temperatures ($700\sim 900^\circ\text{C}$).

From there reasons we consider that the layered sample must return to ambient temperature during processes. In this sense, the sputtering process should take place at half the temperature range of the diamond deposition, allowing cutting in a half value the inescapable game of compressive and tensile residual stresses.

The methane partial pressure value was optimized for the W-C gradient interlayer. Figure 1(a) shows the methane concentration in Ar-CH₄ gas mixtures used in deposition of W-C gradient interlayer on to WC-13%wt.Co substrate. Figure 1(b) shows the cross-sectional SEM images and EDAX spectra of WC-13%wt.Co with a W-C gradient interlayer. For this figure, the cross section was divided into three areas — WC-13%wt.Co substrate zone, tungsten zone and W-C gradient zone. The carbon content of W-C gradient interlayer for interface to surface is gradually increased.

2.2. Diamond deposition

Prior to deposition, tungsten carbide plates have been etched for 60s in mixed weakly acidic solution in an ultrasonic bath, and then cleaned in de-ionized water and acetone for 10 minutes in an ultrasonic bath, respectively. This treatment allows removing contaminant on surface and creating micro-defects at surface. Figure 2 shows the planar and the three-dimensional $3 \times 3 \mu\text{m}^2$ AFM images of W-C gradient layer surface etched by mixed weakly acidic solution. The AFM topographic image shows a randomly distributed rough surface can be formed with 79.612 nm average surface roughness (Ra), 95.832 nm root-mean-square roughness (RMS), 478.971 nm peak to peak distance and 283.917 nm mean grain size.

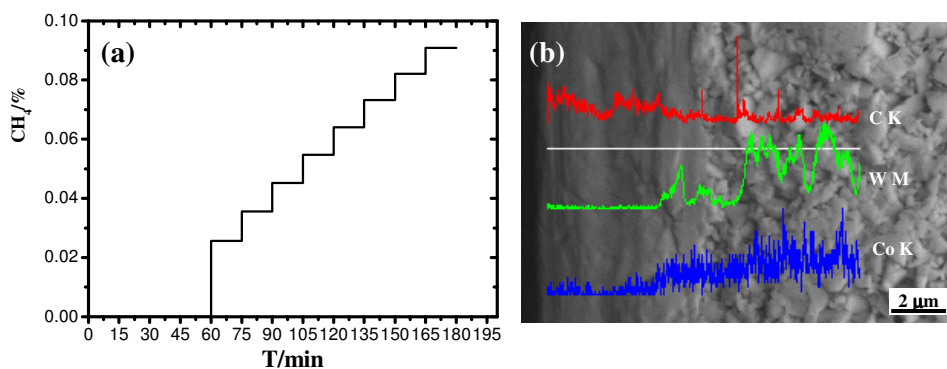


Fig. 1. (a) Methane concentration used in deposition of W-C gradient interlayer on to WC-13%wt.Co; (b) cross-sectional SEM images and EDAX spectra of WC-13%wt.Co with a W-C gradient interlayer.

Then, the samples were treated in an ultrasonic abrasion of acetone suspended with fine diamond powder for 15 minutes. This treatment, usually referred to as “seeding”, allows to enhance the diamond nucleation either by implanting tiny diamond fragments into the substrate surface, on which diamond could subsequently grow during CVD, or by creating suitable defects at the substrate surface, which favor the heterogeneous nucleation of diamond from the gas phase. After this treatment, the samples were cleaned ultrasonically with acetone and ethanol for three times.

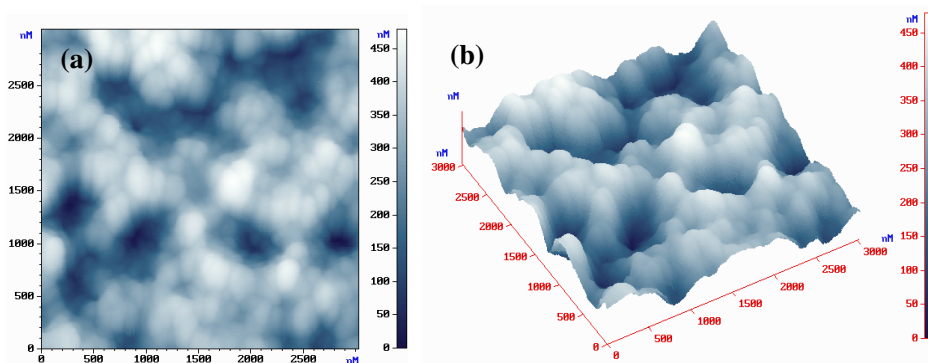


Fig. 2. (a) The planar and (b) the three-dimensional $3 \times 3 \mu\text{m}^2$ AFM images of W-C gradient layer surface.

Prior the nucleation, etching with pure hydrogen was carried out for 10 minutes. During HFCVD of the diamond films, 25 torr pressures and 900°C substrate temperatures were employed. The source gases was CH_4 (99.999% purity), and H_2 (99.999% purity). The experimental details of HFCVD diamond on to WC-13%wt.Co show in Table 1.

Sirion200 FESEM was used to observe the morphology of the W-C gradient interlayers and diamond layers. The roughness Ra and grain size distribution measured by a Solver P47 AFM. XRD patterns have been recorded before and after the diamond deposition by a D/max 2500 XRD diffractometer equipped with a copper X-ray tube ($\lambda_{\text{Cu-K}} = 0.154 \text{ nm}$).

Table 1. Experimental parameters used in deposition of CVD diamond on to WC-13%wt.Co.

Deposition condition	Nucleation	Growth
Substrate temperature (°C)	900	900
CH ₄ /H ₂ (Vol. %)	4	3
Deposition time (min)	15	165
Deposition pressure (torr)	25	25
Total mass flow rate (sccm)	150	150
Filament substrate distance (mm)	9±1	9±1

3. Results and Discussion

3.1. X-ray phase characterization

Figure 3 shows the diffraction peaks of the WC-13%wt.Co substrate, W-C gradient layer and diamond films, respectively. After the deposition of W-C gradient layer X-ray diffraction shows the presence of W and W₂C phase, but no WC diffraction peaks are detected. The result shows that no WC phase was formed during the deposition of W-C gradient layer. Since the thickness of W-C gradient layers are about 10µm, X-ray cannot penetrate through interlayer to detect the WC phase of WC-Co substrate. After the deposition of diamond both WC phases are formed on the samples surface. It is demonstrated that, during HFCVD annealing over 3h at 900°C, the W₂C phases are transformed mainly into WC phases. The intensity of the WC phases shows that the peaks are collected mainly from the intermediate layer and not from the substrate. The diffraction peaks are, however, narrower than that of PVD W-C gradient layer. It is because PVD W-C gradient layer is the very fine structure (nanostructure).

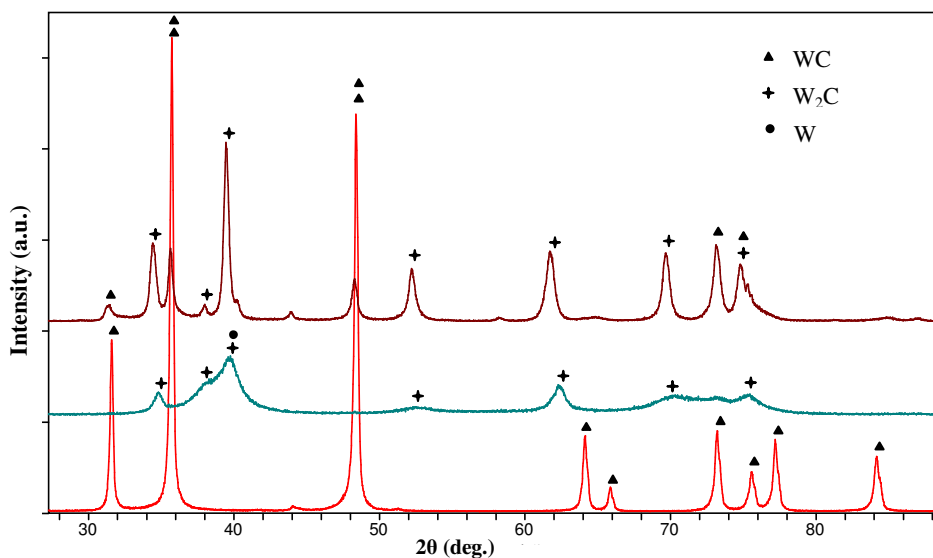


Fig. 3. X-ray diffraction pattern of (a) WC-13%wt.Co, (b) W-C gradient layer, (c) as-deposited diamond film.

3.2. Electron microscopy

Figure 4 shows SEM micrographs of the diamond films grown on WC-13%wt.Co with a W-C gradient interlayer. On both micrographs a fine grained structure can be seen with grain sizes less than 500nm. In Fig. 4, panel (a), the 10000x surface morphology magnified image of diamond films is reported. The figure shows a layer or layers of uniformly and densely distributed nano-scale particles are formed on the substrate. Panel (b) shows the 60000x surface morphology magnified image of diamond films, the clear crystal morphology of diamond grown on WC-13%wt.Co with a W-C gradient interlayer by HFCVD can be identified. Larger magnifications images in panel (b) show the $\langle 100 \rangle \{111\}$ texture of the film and the typical “rough” morphology of the $\{111\}$ facets of CVD diamond.

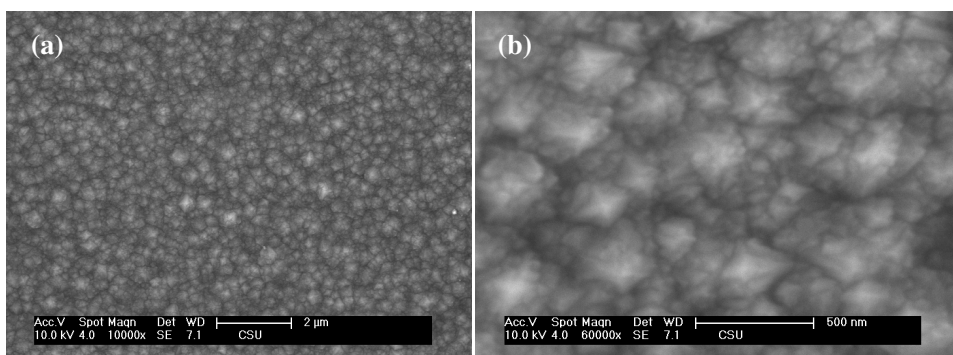


Fig. 4. SEM morphologies of the diamond films grown on WC-13%Co with a W-C gradient interlayer: (a) 10000x; (b) 60000x.

Figure 5 shows AFM images and grain size distribution of diamond films grown on WC-13%wt.Co with a W-C gradient interlayer. The AFM topographic image Fig. 5(a) shows a randomly rough surface with 21.576 nm Ra roughness, 27.008nm RMS roughness, 175.218 nm peak to peak distance and 80.028 nm mean grain size (over the $3 \times 3 \mu\text{m}^2$ area). The AFM grain size distribution of diamond Fig. 5(b) shows nano-scale particles distributed randomly on the surface, the distribution of the size of these particles obeys a Gaussian-like behavior, in another word, the randomness of the size of the particles is identified. The Gaussian peak has a characteristic of peak position at 70nm and its FWHM is around 50nm. The crystal structure is not clearly obtained, due to the small size of these nano-scale particles and large density of diamond. The AFM topographic image also shows layers of uniformly and densely distributed nano-scale particles are formed on the substrate. Therefore, the W-C gradient interlayer pretreatment creates a surface on which the diamond nanopowder particles can distribute themselves densely and uniformly.

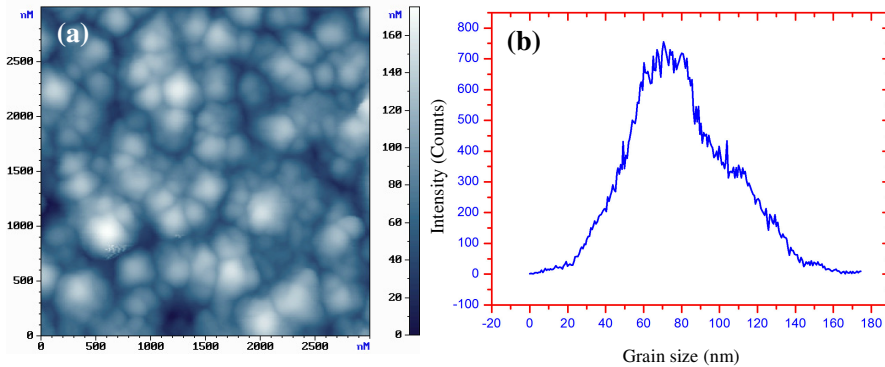


Fig. 5. (a) The planar $3 \times 3 \mu\text{m}^2$ AFM images and (b) the grain size distribution of diamond films grown on WC-13%wt.Co with a W-C gradient interlayer.

Figure 6 shows the XRD pattern of the nanocrystalline diamond films grown on WC-13%wt.Co with a W-C gradient interlayer. (111), (220), (311) and (400) diffraction peaks of diamond were clearly detected at $2\theta=43.8^\circ$, 75.3° , 91.5° , 119.5° and 140.6° , respectively. The diamond (220) peak was overlapped with the intense peak of WC (200) at $2\theta=75.302^\circ \sim 75.477^\circ$.

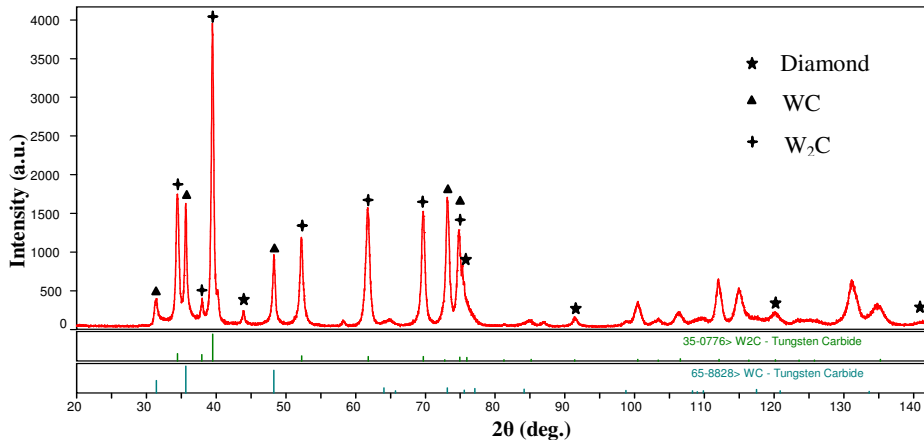


Fig. 6. XRD pattern of the nanocrystalline diamond films grown on WC-13%wt.Co with a W-C gradient interlayer.

4. Conclusion

The W-C gradient interlayers produced via reactive magnetron sputtering can effectively suppress the negative effect of cobalt to diamond films on WC-13%wt.Co comparable to those required for dry machining of highly abrasive materials. W-C gradient intermediate layers can reduce the diffusion of Co during the diamond films deposition process in an effective way, which in turn to obtain high nucleation density and ultra smooth nanocrystalline diamond films. Unlike the classical faceted polycrystalline diamond

coatings, the diamond film obtained using this method display fine-grained morphology with low surface roughness. The creation of a W-C gradient interlayer using diffusion during diamond deposition makes it possible to form strong interfacial bonding between diamond films and substrates. All these results have a variety of possible engineering applications.

Acknowledgments

The authors like to thank “Zhuzhou Cemented Carbide Group Corporation”, “Key State Laboratory of Powder Metallurgy”, “Innovation Foundation for Postgraduate of Hunan Province of China”, and “Open Fund for Valuable Instrument of Central South University” for the financial support.

References

1. K. Vandierendonck, M. Nesládek, S. Kadlec, C. Quaeys, M. V. Stappen, *Surf. Coat. Tech.*, **98**, 1060(1998).
2. F. H. Sun, Z. M. Zhang, M. Chen, H. S. Shen, *J. Mater. Pro. Tech.*, **129**, 435(2002).
3. H. Sein, W. Ahmed, M. Jackson, R. Woodward, R. Polini, *Thin Solid Films*, **447– 448**, 455(2004).
4. G. Cabral, J. Gäbler, J. Lindner, J. Grácio, R. Polini, *Diamond Relat. Mater.*, **17**, 1008 (2008).
5. M. Werner, R. Locher, *Rep. Prog. Phys.*, **61**, 1665(1998).
6. M. Nesládek, K. Vandierendonck, C. Quaeys, M. Kerkhofs, L. M. Stals, *Thin Solid Film*, **270**, 184(1995).
7. A. Inspektor, E. J. Oles, C. E. Bauer, *Int. J. Refract. Met. H.*, **15**, 49(1997).
8. B. Sahoo, A. K. Chattopadhyay, *Diamond Relat. Mater.*, **11**, 1660(2002).
9. S. K. Sarangi, A. Chattopadhyay, A. K. Chattopadhyay, *Appl. Surf. Sci.*, **254**, 3721(2008).
10. S. Silva, V. P. Mammana, M. C. Salvadori, O. R. Monteiro, I. G. Brown, *Diamond Relat. Mater.*, **8**, 1913 (1999).
11. A. Köpf, M. Sommer, R. Haubner, B. Lux, *Diamond Relat. Mater.*, **10**, 790 (2001).
12. Y. S. Lia, Y. Tang, Q. Yang, S. Shimada, R. Wei, K. Y. Lee, A. Hirose, *Int. J. Refract. Met. H.*, **26**, 465(2008).